

Mechanism of chelation of phenanthroline derivatives to Mo(CO)₅ deduced from pulsed photolysis studies in several solvents at high pressure ‡

Shibai Cao, Yanlong Shi, Jens Hollmann, Rudi van Eldik *† and Edward M. Eyring *

Department of Chemistry, University of Utah, Salt Lake City, UT 84112, USA

A laser flash-photolysis kinetic study has been carried out on the concentration, temperature and pressure dependence of chelation reactions of the type $[\text{Mo}(\text{CO})_5(\text{L-L})] \longrightarrow [\text{Mo}(\text{CO})_4(\text{L-L})] + \text{CO}$, where L-L represents 1,10-phenanthroline (phen) and a series of substituted phen ligands in several solvents. The activation parameters for these thermal ring-closure reactions are sensitive to the nature of the solvent, as well as to electronic and steric effects arising from the phen ligand. All the observed kinetic effects can be accounted for by an interchange ligand-substitution mechanism during which CO is displaced by the chelate.

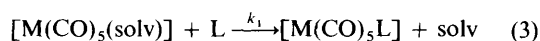
There is continuing interest in details of the mechanism of ligand-substitution reactions of metal carbonyl complexes, especially those of the Group 6 metals owing to their important role in catalytic processes.¹ The photochemical carbonyl substitution of Group 6 metal carbonyls $\text{M}(\text{CO})_6$ (M = Cr, Mo or W) is well established to begin with decarbonylation caused by the absorption of ultraviolet light. The co-ordinatively



unsaturated species thus generated, $\text{M}(\text{CO})_5$, reacts with solvent (solv) and other ligands, L, in subsequent steps (2) and



(3). When the entering nucleophile is a bidentate species L-L



reaction (3) is followed by a slower thermal chelation reaction (4) to give the more stable tetracarbonyl complex. This



chelation involves the displacement of a co-ordinated CO molecule and is of fundamental importance to catalytic cycles involving the binding to and release of molecules from metal centres. Previously available data²⁻⁷ suggest that the nature of the chelation mechanism is controlled by the size of the metal centre (M = Cr, Mo or W) and by steric hindrance at the non-co-ordinated end of the bidentate ligand. Earlier studies⁵ have, for instance, shown that increasing steric hindrance on the bipyridine ligand can cause a changeover from an associative interchange (I_a) to a dissociative interchange (I_d) mechanism for chelation of the corresponding pentacarbonylmolybdenum complexes. The bulky 1,10-phenanthroline (phen) is a significantly more rigid ligand than bipyridine and is expected to

exhibit less flexibility during ring-closure reactions. Thus on treating the smallest metal centre Cr with phen the complex first undergoes loss of CO prior to ring closure according to a dissociative mechanism.⁴ Recently, Oishi⁸ has shown that the interaction of the free N atom of phen with Cr is antibonding and favours such a dissociative mechanism. For the larger metal centres W and Mo we have reported evidence for a more associative ring-closure mechanism.⁵⁻⁷ Clearly, the greatest sensitivity to the steric and electronic properties of the chelate would be expected for the metal centre of intermediate size, *i.e.* Mo. It was found that the molybdenum complexes constitute a case in which an interchange mechanism is operative.^{5,7}

Mechanistic studies of the substitution behaviour of co-ordinated solvent molecules in transition-metal complexes are of fundamental importance to an understanding of the general reactivity patterns of metal complexes in solution. Dobson and co-workers⁹⁻¹¹ have carried out systematic studies of solvent displacement from Group 6 metal carbonyl complexes. The thermal ring-closure reactions of Group 6 metal carbonyls with bidentate ligands have been previously studied^{2,3,5-7} by changing the metals and ligands. In the present study we investigated the solvent effect on the chelate reaction of $[\text{Mo}(\text{CO})_5(\text{phen})]$ by working in a hydrocarbon solvent (heptane), in two aromatic solvents ($\text{C}_6\text{H}_5\text{X}$ where X = Cl or Me), and in the strongly co-ordinating solvent tetrahydrofuran (thf). We have also made a systematic study of the chelation reactions of a series of substituted phenanthroline complexes of the type $[\text{Mo}(\text{CO})_5(\text{L-L})]$. We used, as in our earlier work,^{3-7,9-14} normal- and high-pressure kinetic techniques to resolve the nature of the thermal chelation mechanism. These reactions usually do not involve major changes in electrostriction, since they involve the exchange of neutral molecules. This has made the interpretation of the observed volumes of activation in terms of intrinsic volume changes rather straightforward.^{15,16} Activation volumes obtained from high-pressure kinetic data have been shown to be very sensitive and reliable mechanistic parameters^{17,18} that assist in elucidating the intimate mechanism of chelation processes.

Experimental

Materials

The complex $[\text{Mo}(\text{CO})_6]$ (Aldrich) was vacuum-sublimed before use. 1,10-Phenanthroline (Aldrich), 5-chloro-, 5-nitro-, 4,7-diphenyl- and 2,9-dimethyl-4,7-diphenyl-1,10-phenanthroline (all from Aldrich) were used as received. Heptane and thf (all from Mallinckrodt) were refluxed over Na with

† Present address: Institute for Inorganic Chemistry, University of Erlangen-Nürnberg, 91058 Erlangen, Germany.

‡ Supplementary data available (No. SUP 57127, 5 pp.): experimental first-order rate constants as a function of [phen] in three solvents. See Instructions for Authors, *J. Chem. Soc., Dalton Trans.*, 1996, Issue 1.

benzophenone and distilled under a nitrogen atmosphere. Chlorobenzene (Mallinckrodt) was refluxed over P_2O_5 and distilled under a nitrogen atmosphere. All test solutions were prepared under a nitrogen atmosphere using Schlenk techniques. Solutions were irradiated in quartz pillbox cells and stirred between experiments with the aid of a small Teflon-coated magnetic stirring bar and a magnetic stirrer placed below the high-pressure cell on the optical rail.

Kinetic measurements

The high-pressure, laser flash photolysis ($\lambda = 355$ nm) apparatus and the method of evaluating the experimental kinetic data using KINFIT software from Oligo (Bogart, GA) have both been described previously.⁷ The first-order rate constants, k_{obs} , were obtained by averaging five to ten kinetic traces. The precision in the measurement of activation volume can be expressed¹⁹ by the relative error in ΔV^\ddagger . Volumes of activation were determined from the slopes ($-\Delta V^\ddagger/RT$) of plots of $\ln k_{obs}$ versus pressure, which were all linear with a maximum relative error limit in ΔV^\ddagger of $\pm 13\%$ over the investigated pressure range (0.1–100 MPa).

Results and Discussion

UV/VIS spectra

Irradiation of $[Mo(CO)_6]$ in the presence of a bidentate compound L-L produces the final ring-closed species $[Mo(CO)_4(L-L)]$.^{1a} As noted above, this overall reaction involves the formation of a $Mo(CO)_5$ transient species, that rapidly becomes $[Mo(CO)_5(soln)]$ which in turn becomes the $[Mo(CO)_5(L-L)]$ (ring-opened) species. The existence of each of these species has been demonstrated using flash photolysis, rapid-scan and conventional techniques.^{20–24} Electronic absorption spectra of $[Mo(CO)_4(phen)]$ in different solvents were obtained on a diode-array Hewlett-Packard 8450A UV/VIS spectrophotometer. The assignments are consistent with those reported in other studies.^{22–25} All the thermal ring-closure reactions of $[Mo(CO)_5(phen)]$ were monitored at $\lambda = 490$ nm which is the characteristic metal-to-ligand charge-transfer band of the $[Mo(CO)_4(phen)]$ species. Fig. 1 shows typical kinetic traces recorded at 490 nm following the laser flash in toluene.

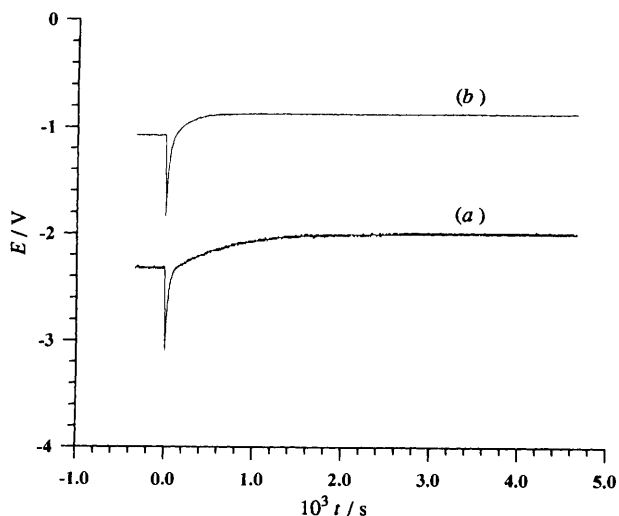


Fig. 1 Typical kinetic traces recorded for the ring-closure reaction $[Mo(CO)_5(phen)] \rightarrow [Mo(CO)_4(phen)] + CO$. Experimental conditions: $[Mo(CO)_6] = 2 \times 10^{-3}$ mol dm⁻³; 25.0 °C; pressure = 0.1 MPa; $\lambda = 490$ nm; $[phen] = 4.5 \times 10^{-3}$ (a) 3.5×10^{-2} mol dm⁻³. (b) The vertical axis represents relative absorbance for which -10 V equals 100% transmission

Solvent effects

Rate constants k_1 for solvent displacement from $[Mo(CO)_5(soln)]$ [Equation(3)] lie in the 10^5 – 10^6 dm³ mol⁻¹ s⁻¹ range with values depending on the solvent and the nature of the entering ligands.^{20,21} Variations in rate constants of the subsequent thermal chelation reactions are partly attributable to steric constraints for the bidentate ligands. In the present solvent studies, k_{obs} has been measured as a function of phen concentrations in toluene, chlorobenzene and heptane. Kinetic data have been deposited as SUP 57127. Plots of k_{obs} versus $[phen]$ in toluene, chlorobenzene and heptane are shown in Figs. 2–4, respectively.

Figs. 2 and 3 show that in toluene and chlorobenzene a straight-line plot of k_{obs} versus $[phen]$ is obtained at low phen concentrations. Upon increasing the ligand concentration, a curved portion emerges gradually that levels off at high phen concentrations. It follows from this plot that we are dealing with a chemical system that undergoes a combination of reaction steps such that the observed rate constant and related activation parameters are composite quantities.

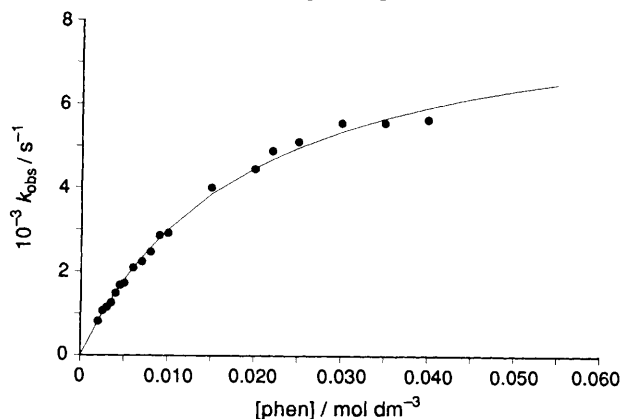


Fig. 2 Plot of k_{obs} versus phen concentration. Experimental conditions: $[Mo(CO)_6] = 2.0 \times 10^{-3}$ mol dm⁻³; solvent = toluene; 25.0 °C; pressure = 0.1 MPa; $\lambda = 490$ nm. The points are experimental data, the line is the fitted curve

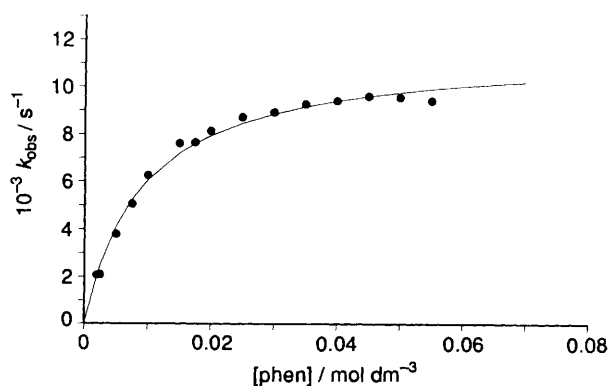


Fig. 3 Plot of k_{obs} versus phen concentration in chlorobenzene. Other details as in Fig. 2

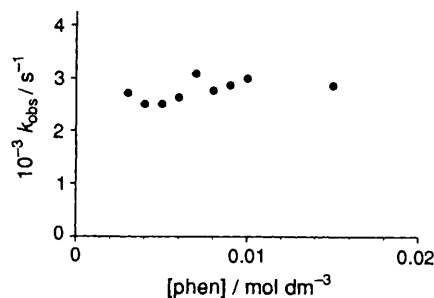


Fig. 4 Plot of k_{obs} versus phen concentration in heptane-toluene (9:1). Other details as in Fig. 2

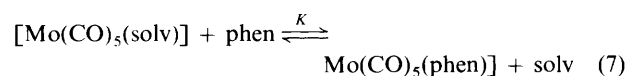
The curved dependence of k_{obs} on [phen] can be interpreted in terms of the mechanism given in equations (1)–(4) with a gradual changeover in the rate-determining step, from solvent displacement at low [phen] to chelation at high [phen]. At low [phen] the solvent displacement is rate-determining, *i.e.* $k_1[\text{phen}] \ll k_2$ and $k_{\text{obs}} = k_1[\text{phen}]$, corresponding to the initial linear part of the plot of k_{obs} versus [phen]. At higher [phen] values the solvent-displacement reaction becomes so fast that the subsequent ring-closure reaction, a concentration-independent step, becomes the rate-determining step, *i.e.* $k_1[\text{phen}] \gg k_2$ and $k_{\text{obs}} = k_2$. Thus the chelate ring-closure reaction obeys the rate law (5), where k_2 is the rate constant for chelate-ring closure.

$$-d[\text{Mo}(\text{CO})_5(\text{L-L})]/dt = k_2[\text{Mo}(\text{CO})_5(\text{L-L})] \quad (5)$$

The experimental data have also been fitted by equation (6)

$$k_{\text{obs}} = a[\text{phen}]/(1 + b[\text{phen}]) \quad (6)$$

using a non-linear least-squares routine, where a and b represent the fitting parameters. The fitted curves are also included as solid lines in Figs. 2 and 3. The experimental data are within the error limits of the fitted curves. This suggests that there may be a rapid pre-equilibrium that involves the solvent-displacement step before the subsequent rate-determining chelation step as shown in equations (7) and (8). The rate law



for this pre-equilibrium mechanism is given in equation (9),

$$k_{\text{obs}} = kK[\text{phen}]/(1 + K[\text{phen}]) \quad (9)$$

which is identical to the empirical rate law (6), with $a = kK$ and $b = K$. It follows that K can be obtained from b and k from the ratio a/b . The chelation rate constants k obtained from this pre-equilibrium model are 8.7×10^3 and $1.3 \times 10^4 \text{ s}^{-1}$ in toluene and chlorobenzene, respectively. These values are higher than the experimental rate constants which are 6.0×10^3 and $9.5 \times 10^3 \text{ s}^{-1}$ respectively obtained at the highest [phen] employed. The resulting values of K are 53 and $110 \text{ dm}^3 \text{ mol}^{-1}$ in toluene and chlorobenzene, respectively. Multiplication of K by the solvent concentration (9.4 for toluene and 9.8 mol dm^{-3} for chlorobenzene) converts these constants into 4.9×10^2 and 1.1×10^3 , respectively. These numbers are the ratios of the rate constants for the formation and dissociation of the $[\text{Mo}(\text{CO})_5(\text{phen})]$ complex produced during the pre-equilibration step (7). These rate constant ratios are quite plausible considering the larger nucleophilicity of phen than those of the solvents employed.

It should be emphasized that the two models, *viz.* the changeover in rate-determining step and the pre-equilibrium treatment, fit the experimental data equally well. The remainder of the discussion will therefore consider both models to account for the observed activation parameters obtained from the effects of temperature and pressure studied at low and high concentrations of phen. In terms of the changeover in rate-determining-step model, both k_1 and k_2 can be determined from the concentration-dependence studies. The temperature and pressure dependence of k_{obs} at low and high [phen] can therefore be used to obtain the activation parameters for k_1 and k_2 respectively. All rate constants and activation parameters for the thermal ring-closure reaction of $[\text{Mo}(\text{CO})_5(\text{phen})]$ in toluene and chlorobenzene are presented in Table 1. Here it

must be kept in mind that $k_{\text{obs}} = k_1[\text{phen}]$ at low [phen], so k_{obs} must be converted into k_1 before ΔH^\ddagger and ΔS^\ddagger can be calculated.

The initial slope of k_{obs} versus [phen] has a value of $4.0 \times 10^5 \text{ dm}^3 \text{ mol}^{-1} \text{ s}^{-1}$ at 25 °C in toluene, thus $k_1 = 4.0 \times 10^5 \text{ dm}^3 \text{ mol}^{-1} \text{ s}^{-1}$ under these conditions. The maximum rate constant at high [phen] corresponds to $k_2 = 6.0 \times 10^3 \text{ s}^{-1}$. Working in benzene at 25 °C, Oishi²⁰ found $k_1 = 8 \times 10^5 \text{ dm}^3 \text{ mol}^{-1} \text{ s}^{-1}$ and $k_2 = 2.4 \times 10^3 \text{ s}^{-1}$ for these same reactants. Kalyanasundaram,²¹ also working in benzene at 25 °C, found $k_1 = 5 \times 10^5 \text{ dm}^3 \text{ mol}^{-1} \text{ s}^{-1}$ and $k_2 = 2.4 \times 10^3 \text{ s}^{-1}$ for these reactants. Thus our results are in good agreement with those reported in the literature. For the solvent-displacement reaction (3) in toluene we find $\Delta H^\ddagger = 33 \pm 1 \text{ kJ mol}^{-1}$ and $\Delta S^\ddagger = -27 \pm 3 \text{ J K}^{-1} \text{ mol}^{-1}$. In the case of reaction (4), $k_{\text{obs}} = k_2$ at high [phen] and the activation parameters found, *i.e.* $\Delta H^\ddagger = 38 \pm 2 \text{ kJ mol}^{-1}$ and $\Delta S^\ddagger = -46 \pm 7 \text{ J K}^{-1} \text{ mol}^{-1}$, are those for thermal ring closure.

In toluene the ΔV^\ddagger value at low [phen] must be that for k_1 . Typical values¹⁰ of ΔV^\ddagger for solvent-displacement reactions of $[\text{Mo}(\text{CO})_5(\text{solv})]$ vary between +2 and +6 $\text{cm}^3 \text{ mol}^{-1}$ for a range of solvents: displacement by hex-1-ene gave $+2.2 \pm 0.3 \text{ cm}^3 \text{ mol}^{-1}$ in heptane, $+5.8 \pm 0.8 \text{ cm}^3 \text{ mol}^{-1}$ in fluorobenzene, $+3.2 \pm 0.3 \text{ cm}^3 \text{ mol}^{-1}$ in chlorobenzene, and $+3.2 \pm 0.3 \text{ cm}^3 \text{ mol}^{-1}$ in toluene, respectively.¹⁰ These small positive ΔV^\ddagger values indicate that solvent displacement follows a dissociative interchange (I_d) type of mechanism. The present value of $+6.1 \pm 0.7 \text{ cm}^3 \text{ mol}^{-1}$ found in toluene (Table 1) falls at one end of the range of values previously reported and indicates that a similar I_d mechanism is operative in the present system. The ΔV^\ddagger value at high [phen] in toluene ($-1.6 \pm 0.1 \text{ cm}^3 \text{ mol}^{-1}$, Table 1) must be related to the chelation process (k_2). The more negative ΔV^\ddagger value found for chelation compared to the solvent-displacement reaction is consistent with the trend in ΔS^\ddagger , indicating that bond formation is more significant during the chelation reaction. This is in agreement with the highly structured nature of the $[\text{Mo}(\text{CO})_5(\text{phen})]$ species that will favour an associative bond-formation process.⁸ Earlier a value of $\Delta V^\ddagger = -2.9 \pm 0.2 \text{ cm}^3 \text{ mol}^{-1}$ was reported⁴ for this reaction in fluorobenzene. The present value in toluene is in reasonable agreement with that found in fluorobenzene, and is more negative than the value of $+0.6 \pm 0.2 \text{ cm}^3 \text{ mol}^{-1}$ reported previously in toluene.⁶ The detailed concentration dependence of k_{obs} determined in the present study confirms that it is only the chelation reaction that is observed at high [phen]. Any interference of the solvent-displacement step when working at lower [phen] will result in a spurious more positive ΔV^\ddagger value attributable to the more positive value found for the solvent-displacement reaction. This probably accounts for the inaccurate solvent displacement ΔV^\ddagger reported earlier in toluene.⁶ Our present value of $-1.6 \pm 0.1 \text{ cm}^3 \text{ mol}^{-1}$ agrees much better with the data reported⁶ for substituted phen ligands in which increasing steric crowding causes a gradual changeover to more positive ΔV^\ddagger values.

In terms of the pre-equilibrium model, the initial slope of the plots of k_{obs} versus [phen] represents kK , which is the product of the pre-equilibrium constant K and the rate-determining chelation k . The reported activation parameters are therefore composite quantities and their interpretation is less straightforward than for the earlier treatment in terms of k_1 . The limiting rate constant reached at high [phen] once again represents the chelation step and the interpretation is similar to that given above for k_2 . The observed volume of activation at low [phen] represents the sum of $\Delta V(K)$, meaning the reaction volume associated with the equilibrium constant K , and $\Delta V^\ddagger(k)$ in terms of the pre-equilibrium model which, combined with the value for $\Delta V^\ddagger(k)$ determined directly at high [phen], results in $\Delta V(K) = \Delta V^\ddagger - \Delta V^\ddagger(k) = +7.7 \pm 0.8$ and $+4.3 \pm 1.9 \text{ cm}^3 \text{ mol}^{-1}$ for toluene and chlorobenzene, respectively. This means that the formation of $[\text{Mo}(\text{CO})_5(\text{phen})]$ is accompanied by an

Table 1 Rate constant k_{obs} as a function of temperature and pressure for the thermal ring-closure reaction of $[\text{Mo}(\text{CO})_5(\text{phen})]$ at low and high $[\text{phen}]$ concentrations in toluene, chlorobenzene and heptane-toluene (9:1)^a

$[\text{L-L}]/\text{mol dm}^{-3}$	$T/^\circ\text{C}$	P/MPa	$10^{-3}k_{\text{obs}}^b/\text{s}^{-1}$	$\Delta H^\ddagger/\text{kJ mol}^{-1}$	$\Delta S^\ddagger/\text{J K}^{-1} \text{mol}^{-1}$	$\Delta V^\ddagger/\text{cm}^3 \text{mol}^{-1}$
Solvent = toluene						
4.5×10^{-3}	10.0	0.1	0.78 ± 0.05	33 ± 1	-27 ± 3	$+6.1 \pm 0.7$
	15.0	0.1	0.98 ± 0.03			
	20.0	0.1	1.28 ± 0.10			
	25.0	0.1	1.68 ± 0.05			
	25.0	20	1.53 ± 0.06			
	25.0	50	1.45 ± 0.09			
3.5×10^{-2}	25.0	100	1.29 ± 0.12	38 ± 2	-46 ± 7	-1.6 ± 0.1
	10.0	0.1	2.32 ± 0.08			
	15.0	0.1	3.23 ± 0.20			
	20.0	0.1	4.36 ± 0.24			
	25.0	0.1	5.55 ± 0.40			
	25.0	20	5.64 ± 0.34			
	25.0	50	5.73 ± 0.36			
	25.0	100	5.98 ± 0.49			
25.0	150	6.13 ± 0.37				
Solvent = chlorobenzene						
5.0×10^{-3}	10.0	0.1	1.84 ± 0.17	32 ± 2	-25 ± 7	-6.7 ± 0.3
	14.0	0.1	2.72 ± 0.08			
	20.0	0.1	3.18 ± 0.23			
	25.0	0.1	3.78 ± 0.22			
	30.0	0.1	5.30 ± 0.80			
	35.0	0.1	6.67 ± 0.89			
	40.0	0.1	7.80 ± 0.77			
	25.0	20	4.03 ± 0.60			
	25.0	50	4.37 ± 0.86			
	25.0	100	4.98 ± 0.67			
5.0×10^{-2}	25.0	0.1	9.56 ± 0.38	-11.0 ± 1.6		
	25.0	20	10.33 ± 0.62			
	25.0	50	12.82 ± 0.43			
	25.0	100	14.77 ± 0.22			
Solvent = heptane-toluene (9:1)						
1.0×10^{-2}	25.0	0.1	2.99 ± 0.17	-3.0 ± 0.1		
	25.0	20	3.08 ± 0.06			
	25.0	50	3.20 ± 0.23			
	25.0	100	3.40 ± 0.16			

^a Experimental conditions: $[\text{Mo}(\text{CO})_6] = 2.0 \times 10^{-3} \text{ mol dm}^{-3}$. ^b Mean value from at least six kinetic traces.

overall small increase in volume, which is rather unexpected since phen displaces the significantly smaller solvent molecule in this equilibrium. A likely reason for the positive reaction volumes is that phen can be highly solvated prior to coordination to the metal centre such that reaction (7) involves significant desolvation of the phen ligand, which will result in an overall volume increase.

For the measurements in heptane, we mixed 90% heptane with 10% toluene in order to improve the solubilities of the reactants in heptane. We compared k_{obs} in pure heptane with that in the toluene-heptane mixture at lower $[\text{phen}]$ and found no significant difference in rate constants. The dependence of k_{obs} on $[\text{phen}]$ was also determined in the mixed solvent. The results shown in Fig. 4 indicate that k_{obs} is independent of $[\text{phen}]$ within the experimental error limits. The rate of solvent displacement from $[\text{Mo}(\text{CO})_5(\text{solv})]$ in heptane is much faster than in toluene, fluorobenzene and chlorobenzene, in agreement with previous studies.¹⁰ Of all these solvents it is reasonable to expect that heptane will be the most weakly co-ordinated, thus accounting for the rapid solvent displacement and the rate-determining chelation step. The $\Delta V^\ddagger = -3.0 \pm 0.1 \text{ cm}^3 \text{ mol}^{-1}$ in heptane also suggests an I_a chelation mechanism in which bond formation is more important than bond breakage, since the solvent molecule is only weakly co-ordinated. Weakly co-ordinating solvents such as toluene, fluorobenzene and heptane in general show faster chelation reactions. The small negative ΔV^\ddagger values are typical for an interchange mechanism.

It is surprising that $\Delta V^\ddagger = -6.7 \pm 0.3 \text{ cm}^3 \text{ mol}^{-1}$ for solvent displacement in chlorobenzene is much more negative than for toluene and is out of the range of values found in earlier studies.¹⁰ In the case of the ring-closure reaction, the ΔV^\ddagger for chlorobenzene is also more negative than that for toluene. For both displacement of CO and subsequent ring closure, chlorobenzene promotes a more associative mechanism as reflected by the more negative ΔV^\ddagger values. This means that in the displacement of chlorobenzene bond formation is more important than bond breakage. This must be related to the bonding mode of this solvent to the Mo which is quite different from those of the rest of the solvents, as expected. This suggests a possible formation of 'head-on' Cl-Mo in the solvated 'ring-opened' intermediate $[\text{Mo}(\text{CO})_4(\text{phen})(\text{C}_6\text{H}_5\text{Cl})]$ instead of 'edgewise' bonding of toluene and fluorobenzene to the Mo. In this case the ring-closure reaction is also characterized by a significantly more negative volume of activation, *viz.* $-11.0 \pm 1.6 \text{ cm}^3 \text{ mol}^{-1}$, indicating the importance of bond formation. This value could even be an indication of the formation of a seven-co-ordinate species $[\text{Mo}(\text{CO})_5(\text{phen})(\text{solv})]$ for systems where the solvent has good co-ordination properties as in the case of chlorobenzene.

In thf the observed rate constant is almost independent of the phen concentration, from which it follows that we are dealing with the chelation process. The rate of chelation is much smaller as seen in Tables 2 and 3. The activation parameters are $\Delta H^\ddagger = 57 \pm 6 \text{ kJ mol}^{-1}$, $\Delta S^\ddagger = -53 \pm 20 \text{ J K}^{-1} \text{ mol}^{-1}$, and $\Delta V^\ddagger = -18.2 \pm 2.2 \text{ cm}^3 \text{ mol}^{-1}$. These large negative ΔS^\ddagger and ΔV^\ddagger

values are consistent with an associative activation process. The ring-closure reaction in thf is orders of magnitude slower than in the other investigated solvents, in agreement with the fact that thf is more strongly co-ordinated than the other solvent molecules and may indicate a 'late' transition state. The more negative value of ΔV^\ddagger indicates a greater volume collapse in the transition state in thf which could be due to a more effective competition between ring closure and co-ordination of thf followed by ring closure in a concerted manner. Previous studies¹¹ of the substitution behaviour of complexes of the type $[\text{Mo}(\text{CO})_5(\text{thf})]$ by piperidine, PPh_3 , and $\text{P}(\text{OEt})_3$ yielded ΔV^\ddagger values of -3.6 ± 1.2 , -8.3 ± 1.0 and $-5.8 \pm 0.9 \text{ cm}^3 \text{ mol}^{-1}$, respectively. Tetrahydrofuran is a much stronger co-ordinating solvent and its reactions tend to follow an I_a mechanism, thus solvent displacement is enforced by the entering nucleophile in a concerted way. From the data in Table 1 it is evident that a stronger co-ordinating solvent like thf slows down the ring-closure reaction and exhibits a more negative ΔV^\ddagger which is similar to that observed for solvent-displacement reactions.¹¹ The phen ligand is highly structured and a direct interaction of the unco-ordinated N donor atom with the metal centre has been suggested, *i.e.* a semi-seven-co-ordinate species. Such an interaction can cause ring closure of phen accompanied by release of CO, or partial labilization of CO so that it can be displaced by a solvent molecule, which is then rapidly displaced by the free end of phen.

Activation volumes for the thermal ring-closure reactions of

Table 2 Rate constant k_{obs} as a function of $[\text{phen}]$ for the reaction^a $[\text{Mo}(\text{CO})_5(\text{L-L})] \longrightarrow [\text{Mo}(\text{CO})_4(\text{L-L})] + \text{CO}$, where L-L = phen, solvent = thf

$[\text{phen}]/\text{mol dm}^{-3}$	$k_{\text{obs}}/\text{s}^{-1}$
2.0×10^{-2}	0.88 ± 0.06
4.0×10^{-2}	0.89 ± 0.08
5.0×10^{-2}	0.92 ± 0.14
6.0×10^{-2}	0.90 ± 0.12

^a Experimental conditions: $[\text{Mo}(\text{CO})_6] = 2.0 \times 10^{-4} \text{ mol dm}^{-3}$, 25.0 °C, $P = 0.1 \text{ MPa}$. ^b Mean value from at least five kinetic traces.

Table 3 Rate constants and activation parameters for chelate ring closure in $[\text{Mo}(\text{CO})_5(\text{phen})]$ in thf^a

$T/\text{°C}$	P/MPa	$k_{\text{obs}}/\text{s}^{-1}$	$\Delta H^\ddagger/\text{kJ mol}^{-1}$	$\Delta S^\ddagger/\text{J K}^{-1} \text{ mol}^{-1}$	$\Delta V^\ddagger/\text{cm}^3 \text{ mol}^{-1}$
12.0	0.1	0.46 ± 0.14	57 ± 6	-53 ± 20	
17.0	0.1	0.55 ± 0.04			
25.0	0.1	0.89 ± 0.08			
30.0	0.1	1.84 ± 0.31			
35.0	0.1	2.43 ± 0.11			
40.0	0.1	3.24 ± 0.48			
25.0	20	1.08 ± 0.04			-18.2 ± 2.2
25.0	50	1.45 ± 0.11			
25.0	100	1.88 ± 0.25			

^a Experimental conditions: $[\text{Mo}(\text{CO})_6] = 2.0 \times 10^{-4} \text{ mol dm}^{-3}$, $[\text{phen}] = 4.0 \times 10^{-2} \text{ mol dm}^{-3}$. ^b Mean value from at least five kinetic traces.

Table 4 Rate constants and activation volumes for the thermal ring-closure reactions of $[\text{M}(\text{CO})_5(\text{L-L})]$ in several solvents, where M = Mo or W and L-L = 1,10-phenanthroline^a

Solvent	k_2/s^{-1} at 0.1 MPa		$\Delta V^\ddagger/\text{cm}^3 \text{ mol}^{-1}$	
	$[\text{Mo}(\text{CO})_5(\text{L-L})]$	$[\text{W}(\text{CO})_5(\text{L-L})]$	$[\text{Mo}(\text{CO})_5(\text{L-L})]$	$[\text{W}(\text{CO})_5(\text{L-L})]$
Toluene	6.0×10^3 ^b	8.8×10^c	-1.6 ± 0.1 ^b	$+3.6 \pm 0.1$ ^c
Fluorobenzene	1.1×10^4 ^b	4.3×10^2 ^c	-2.9 ± 0.2 ^b	-8.2 ± 0.2 ^c
Chlorobenzene	9.5×10^3 ^b	2.2×10^2 ^c	-11.0 ± 1.6 ^b	-5.4 ± 0.2 ^c
Heptane ^d	3.0×10^3 ^b	7.3×10^c	-3.0 ± 0.1 ^b	-4.0 ± 0.2 ^c
Tetrahydrofuran	8.9×10^{-1} ^b	1.7×10^2 ^c	-18.2 ± 2.2 ^b	-14.9 ± 0.8 ^c

^a $T = 25.0 \text{ °C}$. ^b This work. ^c Ref. 25. ^d heptane-toluene (9:1).

$[\text{W}(\text{CO})_5(\text{phen})]$ in several solvents have been reported.²⁶ The activation volumes of the thermal ring-closure reaction in the weakly co-ordinated solvents, namely toluene, fluorobenzene, heptane and chlorobenzene (see Table 4) are in many cases rather small. For comparison, the thermal ring-closure reaction of $[\text{W}(\text{CO})_5(\text{phen})]$ in strongly co-ordinated tetrahydrofuran solvent has been determined in the present study. The larger negative value of $\Delta V^\ddagger = -14.9 \pm 0.8 \text{ cm}^3 \text{ mol}^{-1}$ resembles that of $-18.2 \pm 2.2 \text{ cm}^3 \text{ mol}^{-1}$ found for $[\text{Mo}(\text{CO})_5(\text{phen})]$ dissolved in thf in the present study. Since ΔV^\ddagger is decidedly different for thf as solvent compared to any of the other solvents studied that are more weakly co-ordinating, it appears that the thf solvent molecule is more heavily involved in the thermal ring-closure mechanism for both of these metals. This is ascribed to a more effective competition between ring closure and co-ordination of thf to produce a seven-co-ordinate intermediate followed by ring closure in a concerted manner.

Substituent effects

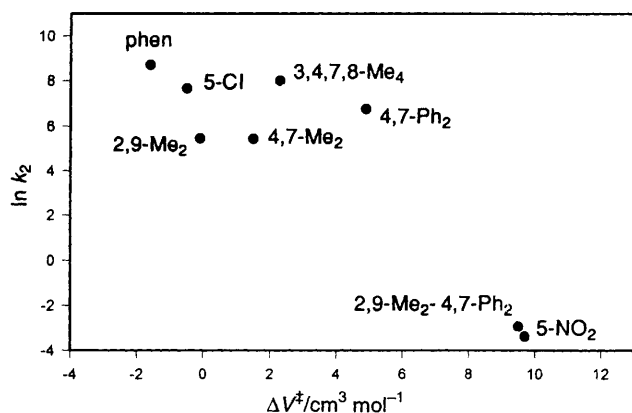
The values of k_2 in toluene measured as a function of pressure for a series of substituted 1,10-phenanthrolines are shown in Table 5. A plot of $\ln k_2$ versus ΔV^\ddagger for chelation of 1,10-phenanthroline and its derivatives is shown in Fig. 5. Substituents on phen can cause steric and electronic effects in the chelation reactions. All the observed rate constants are smaller than for unsubstituted phen due to these effects. From a comparison of the $\text{p}K_a$ values for pyridine and aniline with those for substituted species it is known²⁷ that the $\text{p}K_a$ values all decrease after introduction of electron-withdrawing groups. For example, $\text{p}K_a$ for pyridine is 5.25 at 25 °C, but for 4-chloropyridine $\text{p}K_a$ is 2.84. For aniline $\text{p}K_a$ is 4.63 at 25 °C. Introduction of electron-withdrawing groups, such as benzyl, bromo, chloro and nitro, at different positions on aniline yields $\text{p}K_a$ values of 2.17 (4-benzyl), 2.53 (2-bromo), 4.15 (4-chloro), 3.46 (3-chloro), 2.46 (3-nitro) and 1.0 (4-nitro), respectively. The lower $\text{p}K_a$ values mean a decrease in basicity and nucleophilicity of the substituted anilines. Introduction of electron-withdrawing substituents (*viz.* Cl and NO_2) will decrease the electron density on phen such that the donor N atoms will be less basic. The basicity of the N donor atoms will control the nucleophilicity and the rates of the ring-closure reactions.

With regard to steric effects, introduction of substituents in the 2 and 9 positions of phen can be crucial for the ring-closure reaction. Methyl substituents in these positions will cause an increase in electron density on the N atoms and consequent higher basicity, such that steric and electronic effects may cancel out. Steric effects at the 4 and 7 positions are expected to be less important, but larger groups such as Ph may have a larger effect. We have found that k_2 is very similar in most cases (see Table 5). For instance, the reactions of 2,9- and 4,7-dimethylphenanthroline seem to be a bit slower than for phen and are also characterized by slightly more positive ΔV^\ddagger values. 4,7-Diphenylphenanthroline also shows a slower reaction and a more positive ΔV^\ddagger . The largest effects are seen for Me_2Ph_2

Table 5 Rate constants and activation volumes for chelate ring closure in $[\text{Mo}(\text{CO})_5(\text{L-L})]$ complexes in toluene^a

$[\text{Mo}(\text{CO})_5]/\text{mol dm}^{-3}$	L-L (λ/nm^b)	$[\text{L-L}]/\text{mol dm}^{-3}$	P/MPa	$k_{\text{obs}}^c/\text{s}^{-1}$	$\Delta V^\ddagger/\text{cm}^3 \text{mol}^{-1}$
2.0×10^{-4}	dpphen (500)	2.0×10^{-3}	0.1	$(8.98 \pm 0.14) \times 10^2$	$+4.9 \pm 0.4$
			20	$(8.52 \pm 1.52) \times 10^2$	
			50	$(7.96 \pm 0.23) \times 10^2$	
			100	$(7.06 \pm 0.25) \times 10^2$	
2.0×10^{-3}	dmpphen (500)	1.0×10^{-2}	0.1	$(5.30 \pm 0.60) \times 10^{-2}$	$+9.5 \pm 0.6$
			20	$(5.07 \pm 0.55) \times 10^{-2}$	
			50	$(4.41 \pm 0.42) \times 10^{-2}$	
			100	$(3.63 \pm 0.33) \times 10^{-2}$	
1.0×10^{-3}	nphen (510)	1.0×10^{-2}	0.1	$(3.43 \pm 0.45) \times 10^{-2}$	$+10.3 \pm 1.2$
			20	$(3.29 \pm 0.34) \times 10^{-2}$	
			50	$(2.70 \pm 0.31) \times 10^{-2}$	
			100	$(2.30 \pm 0.14) \times 10^{-2}$	
2.0×10^{-4}	cphen (500)	1.0×10^{-2}	0.1	$(2.09 \pm 0.39) \times 10^3$	-1.2 ± 0.1
			20	$(2.11 \pm 0.34) \times 10^3$	
			50	$(2.14 \pm 0.17) \times 10^3$	
			100	$(2.20 \pm 0.14) \times 10^3$	

^a At 25.0 °C. Abbreviations used: dpphen = 4,7-diphenyl-1,10-phenanthroline; dmpphen = 2,9-dimethyl-4,7-diphenyl-1,10-phenanthroline; nphen = 5-nitro-1,10-phenanthroline; cphen = 5-chloro-1,10-phenanthroline. ^b Wavelengths of metal-to-ligand charge-transfer bands of the $[\text{Mo}(\text{CO})_5(\text{L-L})]$ complexes where reactions were monitored are given in parentheses. ^c Mean value of at least 5 kinetic traces.

**Fig. 5** Plot of $\ln k_2$ versus ΔV^\ddagger for the chelation of phen and its substituted derivatives when bound to $\text{Mo}(\text{CO})_5$ in toluene**Table 6** Summary of rate constants (0.1 MPa) and activation volumes for ring-closure reactions of $[\text{Mo}(\text{CO})_5(\text{L-L})]$ complexes

Solvent	L ^a	k_2 (25° C)/s ⁻¹	$\Delta V^\ddagger/\text{cm}^3 \text{mol}^{-1}$	Ref.
C_6H_6	phen	5.6×10^3	—	15
$\text{C}_6\text{H}_5\text{Me}$	phen	6.0×10^3	-1.6 ± 0.1	<i>b</i>
$\text{C}_6\text{H}_5\text{F}$	phen	1.1×10^4	-2.9 ± 0.2	4
$\text{C}_6\text{H}_5\text{Cl}$	phen	9.6×10^3	-11.0 ± 1.6	<i>b</i>
^c	phen	3.0×10^3	-3.0 ± 0.1	<i>b</i>
thf	phen	8.9×10^1	-18.2 ± 2.2	<i>b</i>
$\text{C}_6\text{H}_5\text{Me}$	2,9-dmphen	2.4×10^2	-0.1 ± 0.4	6
$\text{C}_6\text{H}_5\text{Me}$	4,7-dmphen	2.3×10^2	$+1.5 \pm 0.3$	6
$\text{C}_6\text{H}_5\text{Me}$	tmphen	3.0×10^3	$+2.3 \pm 0.4$	6
$\text{C}_6\text{H}_5\text{Me}$	dpphen	9.0×10^2	$+4.9 \pm 0.4$	<i>b</i>
$\text{C}_6\text{H}_5\text{Me}$	dmpphen	5.3×10^{-2}	$+9.5 \pm 0.6$	<i>b</i>
$\text{C}_6\text{H}_5\text{Me}$	nphen	3.4×10^{-2}	$+10.3 \pm 1.2$	<i>b</i>
$\text{C}_6\text{H}_5\text{Me}$	cphen	2.1×10^3	-1.2 ± 0.1	<i>b</i>

^a dmphen = Dimethyl-1,10-phenanthroline, tmphen = 3,4,7,8-tetra-methyl-1,10-phenanthroline. ^b This work. ^c Heptane-toluene (9:1).

and NO_2 substituents; both reactions are very slow and characterized by large positive ΔV^\ddagger values. In the case of Me_2Ph_2 the effect must be mainly steric due to a combination of both Me and Ph as substituents. A comparable effect is not seen for only Me or only Ph as substituents. In the case of NO_2 , there must be an electronic effect due to its strong electron-withdrawing ability. The phen N donor is much less basic (lower $\text{p}K_a$) and causes the chelation reaction to be slower. The slower reaction seems to be controlled by the release of CO, thus either steric hindrance or basicity can prevent an associative chelation (I_a) mechanism and can cause a changeover to a more dissociative (I_d) mechanism. This trend from more negative to more positive ΔV^\ddagger values in going from faster to slower ring-closure reactions also demonstrates the position of the transition state along the reaction coordinate in terms of being 'early' or 'late'. For faster reactions, ring closure will occur prior to the release of CO (*i.e.* negative ΔV^\ddagger , I_a), whereas the slower reactions will involve more carbonyl bond cleavage (*i.e.* positive ΔV^\ddagger , I_d). The 'early' transition state will be closer to the reactant structure in terms of semi-seven-co-ordination, and the 'late' one will be closer to the product state, *i.e.* chelated and total release of CO.

A summary of the available rate and activation volume data for ring-closure reactions of $[\text{Mo}(\text{CO})_5(\text{L-L})]$ complexes in different solvents, where L-L represents a series of substituted

1,10-phenanthroline ligands, is given in Table 6. These values indicate that $[\text{Mo}(\text{CO})_5(\text{phen})]$ undergoes ring closure according to an associative interchange (I_a) mechanism which can gradually change to an I_d mechanism with increasing steric hindrance on the phen ligand. The faster ring-closure reactions show ΔV^\ddagger values between -2 and $+5 \text{ cm}^3 \text{mol}^{-1}$ typical of an interchange mechanism. The slower reactions exhibit more positive ΔV^\ddagger values (see Fig. 5), indicating that chelation is probably controlled by the release of CO. The chelation rates are also controlled by the basicity of these substituted phen ligands. It has been suggested that the highly structured nature of the phen ligand compared to bipyridine will cause the free end of phen in $[\text{Mo}(\text{CO})_5(\text{phen})]$ to be close to the metal centre.⁶ This can be visualized as an encounter situation that facilitates the associative interchange of ligands. Naturally, the electronic effects and steric hindrance will influence this encounter interaction and force the mechanism to change gradually to a more dissociative interchange of ligands.

We conclude that the steric and electronic properties of the bidentate ligand and the co-ordinating abilities of the solvent play an important role in determining the location of the transition state along the reaction coordinate for the chelation reaction of $[\text{Mo}(\text{CO})_5(\text{phen})]$. The activation parameter ΔV^\ddagger is especially helpful in revealing the intimate mechanism of this reaction.¹⁴

Acknowledgements

This work was supported in part by grants from the Department of Energy, Office of Basic Energy Sciences (to E. M. E.) and the Volkswagen Foundation (to R. v. E.).

References

- (a) G. L. Geoffroy and M. S. Wrighton, *Organometallic Photochemistry*, Academic Press, New York, 1979; (b) T. J. Meyer and J. V. Caspar, *Chem. Rev.*, 1985, **85**, 187; (c) A. E. Stiegman and D. R. Tyler, *Coord. Chem. Rev.*, 1985, **63**, 217.
- K. B. Reddy and R. van Eldik, *Inorg. Chim. Acta*, 1990, **169**, 13.
- K. B. Reddy and R. van Eldik, *Organometallics*, 1990, **9**, 1418.
- S. Zhang, V. Zang, G. R. Dobson and R. van Eldik, *Inorg. Chem.*, 1991, **30**, 355.
- K. B. Reddy, R. Hoffmann, G. Konya, R. van Eldik and E. M. Eyring, *Organometallics*, 1992, **11**, 2319.
- K. B. Reddy, B. R. Brady, E. M. Eyring and R. van Eldik, *J. Organomet. Chem.*, 1992, **440**, 113.
- S. Cao, K. B. Reddy, E. M. Eyring and R. van Eldik, *Organometallics*, 1994, **13**, 91.
- S. Oishi, *Coord. Chem. Rev.*, 1994, **132**, 161.
- S. Zhang, H. C. Bajaj, V. Zang, G. R. Dobson and R. van Eldik, *Organometallics*, 1992, **11**, 3901.
- V. Zang, S. Zhang, C. B. Dobson, G. R. Dobson and R. van Eldik, *Organometallics*, 1992, **11**, 1154.
- S. Zhang and G. R. Dobson, *Organometallics*, 1992, **11**, 2447.
- S. Zhang, G. R. Dobson, H. C. Bajaj, V. Zang and R. van Eldik, *Inorg. Chem.*, 1990, **29**, 3477.
- S. Zhang, V. Zang, H. C. Bajaj and R. van Eldik, *J. Organomet. Chem.*, 1990, **397**, 279.
- S. Wieland and R. van Eldik, *Organometallics*, 1991, **10**, 3110.
- Y. Ducommun and A. E. Merbach, *Inorganic High Pressure Chemistry: Kinetics and Mechanisms*, ed. R. van Eldik, Elsevier, Amsterdam, 1986, ch. 2.
- J. W. Akitt and A. E. Merbach, *NMR Basic Principles and Progress*; Springer, Berlin, Heidelberg, 1990, vol. 24, p. 189.
- R. van Eldik and A. E. Merbach, *Comments Inorg. Chem.*, 1992, **12**, 341.
- R. van Eldik, *Perspectives in Coordination Chemistry*, eds. A. F. Williams, C. Floriani and A. E. Merbach, VCH, Basel and Weinheim, 1992, p. 55.
- S. W. Benson, *The Foundation of Chemical Kinetics*, McGraw-Hill, New York, 1960, p. 91.
- S. Oishi, *Organometallics*, 1988, **7**, 1237.
- K. Kalyanasundaram, *J. Phys. Chem.*, 1988, **92**, 2219.
- M. J. Schadt and A. J. Lees, *Inorg. Chem.*, 1986, **25**, 672.
- D. E. Marx and A. J. Lees, *Inorg. Chem.*, 1987, **26**, 2254.
- D. P. Drolet, L. Chan and A. J. Lees, *Organometallics*, 1988, **7**, 2502.
- D. E. Marx and A. J. Lees, *Inorg. Chem.*, 1987, **26**, 620.
- Q. Ji, E. M. Eyring, R. van Eldik, K. P. Johnston, S. R. Goates and M. L. Lee, *J. Phys. Chem.*, 1995, **99**, 13 461.
- Handbook of Chemistry and Physics*, 6th edn, CRC Press, Cleveland, OH, 1979–1980, p. D161.

Received 21st August 1995; Paper 5/05527J